Human Molecular Genetics, 2014, Vol. 23, No. 5 ***1237–1249***
doi:10.1093/hmg/ddt514
Advance Access published on October 24, 2013

Restoration of muscle strength in dystrophic muscle by angiotensin-1-7 through inhibition of TGF-β signalling

María José Acuña[1], Patrizia Pessina[2], Hugo Olguin[1], Daniel Cabrera[1], Carlos P. Vio[1], Michael Bader[3], Pura Muñoz-Canoves[2], Robson A. Santos[4], Claudio Cabello-Verrugio[1,†] and Enrique Brandan[1,*]

[1]Center for Aging and Regeneration, CARE Chile UC and Department Cell and Molecular Biology, Faculty of Biological Sciences, Catholic University of Chile, Santiago, Chile, [2]Cell Biology Group, Department of Experimental and Health Sciences, Pompeu Fabra University, ICREA and CIBERNED, 08003 Barcelona, Spain, [3]Max-Delbrück-Center for Molecular Medicine (MDC), Berlin-Buch, Berlin, Germany and [4]Department of Physiology and Biophysics, Biological Sciences Institute, INCT Nanobio-far, Federal University of Minas Gerais, 31270-901 Belo Horizonte, MG, Brazil

Received August 12, 2013; Revised October 7, 2013; Accepted October 14, 2013

Duchenne muscular dystrophy (DMD) is the most common inherited neuromuscular disease, and is characterized by the lack of dystrophin, muscle wasting, increased transforming growth factor (TGF)-β Smad-dependent signalling and fibrosis. Acting via the Mas receptor, angiotensin-1-7 [Ang-(1-7)], is part of the renin–angiotensin system, with the opposite effect to that of angiotensin II. We hypothesized that the Ang-(1-7)/Mas receptor axis might protect chronically damaged tissues as in skeletal muscle of the DMD mouse model *mdx*. Infusion or oral administration of Ang-(1-7) in *mdx* mice normalized skeletal muscle architecture, decreased local fibrosis and improved muscle function *in vitro* and *in vivo*. These positive effects were mediated by the inhibition of TGF-β Smad signalling, which in turn led to reduction of the pro-fibrotic microRNA miR-21 concomitant with a reduction in the number of TCF4 expressing fibroblasts. *Mdx* mice infused with Mas antagonist (A-779) and *mdx* deficient for the Mas receptor showed highly deteriorated muscular architecture, increased fibrosis and TGF-β signalling with diminished muscle strength. These results suggest that this novel compound Ang-(1-7) might be used to improve quality of life and delay death in individuals with DMD and this drug should be investigated in further pre-clinical trials.

INTRODUCTION

Duchenne muscular dystrophy (DMD), caused by mutations in the dystrophin gene on the X chromosome, is one of the most common inherited neuromuscular diseases, affecting 1 in 3500 male births. Dystrophin, the dystrophin-associated glycoprotein complex, and laminin α-2 form a link between the extracellular matrix and the intracellular cytoskeleton; this link is crucial for maintaining the structural integrity of muscle fibres (1,2). The main consequences of a lack of dystrophin in skeletal muscle are sarcolemmal instability and increased fibre vulnerability to mechanical stress, resulting in fibre degeneration, followed to some extent by regeneration. However, complete regeneration is prevented by fibrosis (proliferation of connective tissue), which progressively replaces muscle tissue (3–5). Fibrosis is a complex and incompletely understood process characterized by the excessive accumulation of collagens and other extracellular matrix components (6). It occurs under chronic disease conditions and affects various tissues and organs (7).

Angiotensin-1-7 [Ang-(1-7)] is a novel endogenous bioactive peptide metabolite derived mainly from angiotensin II, with important effects, including vasodilation (8,9), inhibition of cell proliferation (10–12) and antihypertensive (13) and antiarrhythmic (14) effects. In addition, Ang-(1-7) has been implicated in

*To whom correspondence should be addressed. Email: ebrandan@bio.puc.cl
†Present address: Laboratorio de Biología y Fisiopatología Molecular, Facultad de Ciencias Biológicas & Facultad de Medicina, Departamento de Ciencias Biológicas, Universidad Andres Bello, Sazié Santiago, Chile.

the protection of tissues from chronic injury through direct effects on tissue fibrogenesis (11,12). The effects of Ang-(1-7) are mediated by the Mas receptor (15,16).

Transforming growth factor type-β (TGF-β) is a central mediator of fibrogenesis that is upregulated and stimulated in fibrotic diseases (6,17) acting directly or through other growth factor mediators (18). Previous studies have shown that the administration of losartan, an Ang II type 1 receptor blocker (ARB), inhibits increased TGF-β signalling activity, with the signal being transduced through the Smad intracellular signalling cascade (19), promotes muscle remodelling in mouse models of Marfan syndrome and DMD (20) and provides protection against disuse or atrophy in humans with sarcopenia (21). Here, we show that infusion of Ang-(1-7) normalizes *mdx* mice skeletal muscle architecture, diminishes fibrosis and improves function *in vivo*. Through pharmacological and genetic evidence, we determined that the positive effects of Ang-(1-7) observed in the dystrophic mice are associated with an inhibition of TGF-β-Smad-dependent signalling through the Mas receptor.

RESULTS

Ang-(1-7) restored muscle architecture, decreased fibrosis and increased skeletal muscle force in *mdx* mice

To evaluate the role of Ang-(1-7) on TGF-β induced fibrosis, wild-type mice were infused with Ang-(1-7) using osmotic pumps for 12 days and the tibialis anterior (TA) skeletal muscle injected with TGF-β for 24 h (22). We observed a decrease amount of fibronectin and connective tissue growth factor (CTGF/CCN2) in response to TGF-β in TA as a consequence of Ang-(1-7) infusion compared to the saline infused animals (Supplementary Material, Fig. S1A–C), suggesting that Ang-(1-7) inhibited the pro-fibrotic effects of TGF-β. Therefore, we decided to evaluate the effect of Ang-(1-7) in *mdx* mice, characterized by an elevated fibrosis and TGF-β mediated signalling (20). Since *mdx* mice present an active skeletal muscle regenerative process, all experiments except those using aged mice were conducted under an exercise protocol to accelerate the onset of fibrosis in the hindlimbs (23) (Supplementary Material, Fig. S2A–C). To evaluate the effect of Ang-(1-7) on the *mdx* skeletal muscle phenotype *in vivo*, we infused Ang-(1-7) using osmotic pumps beginning at 12 weeks of age. After 4 weeks of infusion, histological assessment showed an improvement in the skeletal muscle morphology, indicating a substantial decrease in the amount of inflammatory tissue and fibrosis around individual fibres in the gastrocnemius (GM) (Fig. 1A) and TA skeletal muscle (Supplementary Material, Fig. S3A). Ang-(1-7) infusion considerably reduced the amount of total collagen (Fig. 1B and C) and collagen type I, III and fibronectin in the endomysium and perymisium of *mdx* GM (Fig. 1D) and TA (Supplementary Material, Fig. S3B). Western blot analyses showed a decrease in the amount of fibronectin and collagen type III present in diaphragm skeletal muscle (DIA) as a consequence of Ang-(1-7) infusion (Fig. 1E and F). Analysis of the diameter of GM fibres indicated no significant changes in *mdx* infused with Ang-(1-7) compared with *mdx* mice (Supplementary Material, Fig. S3C).

We next determined whether *mdx* treatment with Ang-(1-7) has a beneficial impact on muscle function. A running test on a treadmill showed a significant improvement of exercise performance, as assessed in the treadmill tests compared with *mdx* (Fig. 1G). Next, we analyzed the physiological properties of DIA derived from wild-type, *mdx* and Ang-(1-7)-infused animals. The explanted DIA from Ang-(1-7)-treated *mdx* mice generated significantly more absolute force over a wide range of stimulation frequencies (30–200 Hz) when compared with untreated *mdx* mice (Fig. 1H). It has been established that fibrosis and muscle damage increase with age (24,25) (Supplementary Material, Fig. S2D–F), and therefore we evaluated whether Ang-(1-7) was also effective in old animals. Eight-month-old *mdx* mice received Ang-(1-7) for 2 months. At the end of treatment, assessment of GM histology indicated a substantial structural improvement compared with *mdx* mice without the treatment (Supplementary Material, Fig. S4A). Levels of total collagen (Supplementary Material, Fig. S4B and C), fibronectin (Supplementary Material, Fig. S4D) and specific collagen III decreased significantly (Supplementary Material, Fig. S4E and F). Finally, we determined the performance of the Ang-(1-7)-treated *mdx* mice on a treadmill; treatment significantly decreased the number of detentions during the test to values even lower than those of wild-type animals (Supplementary Material, Fig. 4G). These observations indicate that Ang-(1-7) also has beneficial effects on skeletal muscle structure, fibrosis and physiology of young and old animals.

Delivery of Ang-(1-7) included in hydroxypropyl β-cyclodextrin (CD-Ang-(1-7)) present beneficial effects in muscle architecture and muscle function

To provide further evidence on the effect of Ang-(1-7), and to deliver the peptide in a suitable way regarding to possible future therapeutics, the peptide was delivered to mice in hydroxypropyl β-cyclodextrin (CD-Ang-(1-7)) via gavage for 4 weeks (26). Histological analyses of GM, TA and DIA showed a substantial improvement (Fig. 2A) together with a decrease in total collagen staining (Fig. 2B and C) and collagen III levels (Fig. 2D and E). We next determined whether *mdx* treatment with (CD-Ang-(1-7)) has a beneficial impact on muscle function. A running test on a treadmill showed a significant improvement of exercise performance, as assessed in the treadmill tests compared with *mdx* (Fig. 2F).

A potent antagonist of Ang-(1-7) receptor impaired dystrophic muscle histology, increased fibrosis and worsened skeletal muscle force in *mdx*

Ang-(1-7) acts primarily through the Mas receptor. To determine whether the above beneficial effects observed in the *mdx* mice were mediated by this receptor, we infused *mdx* mice with A-779, a potent antagonist of the Mas receptor (27). Treatment of *mdx* mice with A-779 significantly deteriorated the GM and DIA as determined by the histological analysis (Fig. 3A, Supplementary Material, Fig. S5A), together with an increase in total collagen (Fig. 3B and C), collagen type I, III and fibronectin (Fig. 3D, and Supplementary Material, Fig. S5B). Western blot analyses showed an increase in the amount of fibronectin in A-779-treated GM compared with untreated *mdx* (Fig. 3E and F). At the physiological level, the infusion of A-779 into *mdx* mice showed a significant poor exercise performance, as

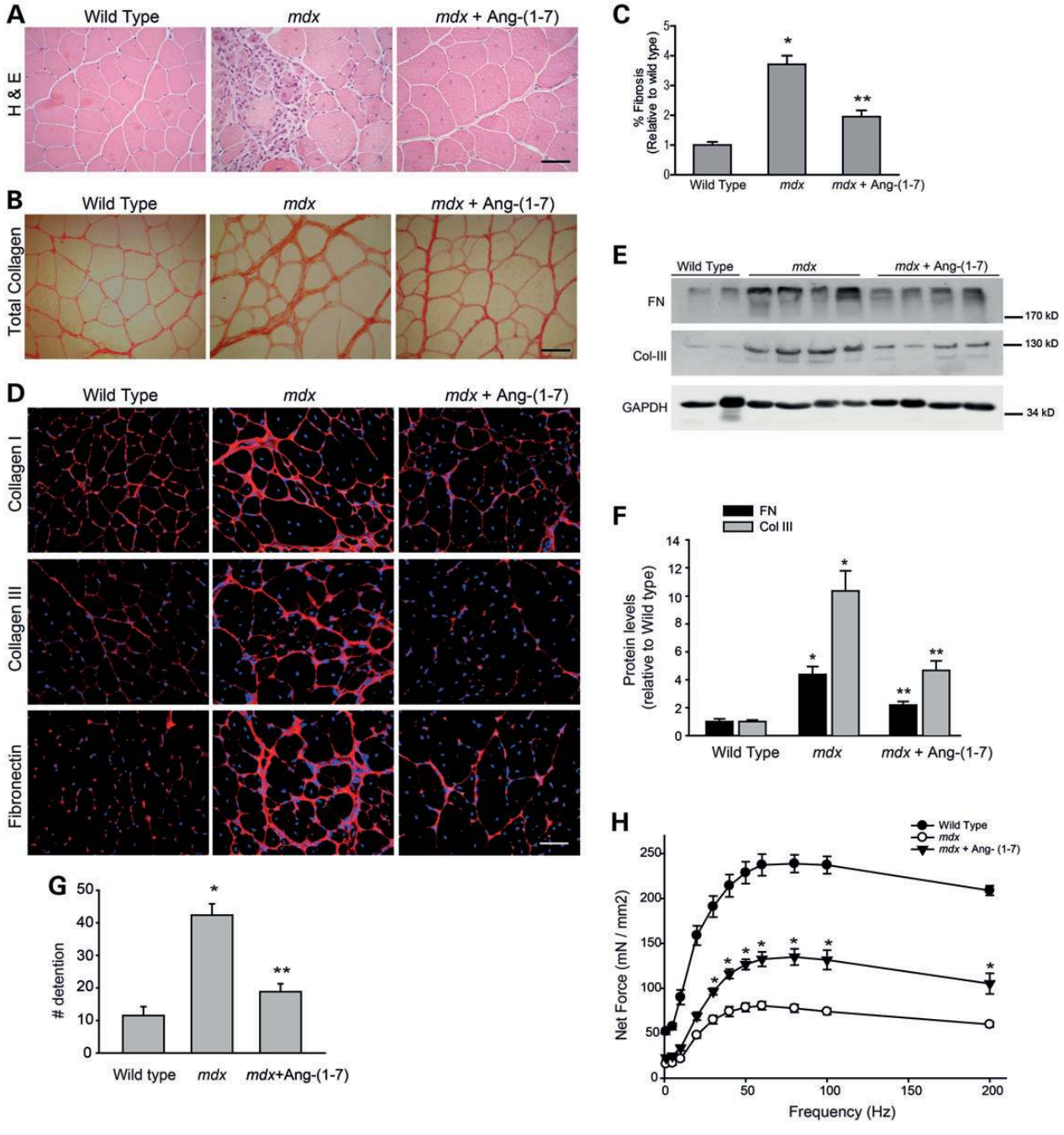

Figure 1. Ang-(1-7) restored muscle architecture, decreased fibrosis and increased skeletal muscle force in *mdx* mice. Twelve weeks old mice were treated with Ang-(1-7) by systemic infusion for 2 months and tissue was collected at this time. (**A**) Ang-(1-7) significantly improved GM *mdx* skeletal muscle architecture, compared with untreated *mdx* evidenced by haematoxylin eosin staining. (**B**) Sirius red staining was reduced and showed improved architecture of *mdx* GM muscle after Ang-(1-7) infusion. (**C**) Quantitation of fibrosis area of 10 fields of Sirius red photographs $n = 4$ animals per group. One-way ANOVA, $^{*}P < 0.001$wild-type versus *mdx*, $^{**}P < 0.001$ *mdx* versus *mdx* + Ang-(1-7). (**D**) The extent of fibrosis (indicated by collagen type I, III and fibronectin staining) was greatly reduced in GM after Ang-(1-7) infusion. (**E**) Western blot analysis of a total DIA protein extract showing fibronectin and collagen reduction after Ang-(1-7) infusion ($n = 4$), and in untreated *mdx* ($n = 4$) and wild-type ($n = 3$) mice. (**F**) Levels of fibronectin and collagen type III were quantified using relative expression compared with wild-type. One-way ANOVA, $^{*}P < 0.001$ wild-type versus *mdx*, $^{**}P < 0.01$ *mdx* versus *mdx* + Ang-(1-7). (**G**) *Mdx* mice treated with Ang-(1-7) performed better in a treadmill test compared with untreated *mdx* mice. One way ANOVA, $^{*}P < 0.001$ wild-type versus *mdx*, $^{**}P < 0.001$ *mdx* versus *mdx* + Ang-(1-7). (**H**) *In vitro* force–frequency relationship of explanted DIA muscle: isometric net force normalized to muscle CSA (relative tension) versus stimulation frequency (1–200 Hz) increased in Ang-(1-7)-infused *mdx* mice at frequencies equal to or greater than 30 Hz, in comparison with untreated *mdx* mice. Two-way ANOVA, $^{*}P < 0.001$ *mdx* versus *mdx* + Ang-(1-7) ($n = 8$ animals). Scale bar, 50 μm.

assessed in the treadmill tests compared with *mdx* (Fig. 3G). The absolute force of explanted DIA obtained from *mdx* mice infused with the Mas antagonist was determined. The net force dropped significantly compared with *mdx* across a wide range of stimulation frequencies (30–80 Hz) (Fig. 3H). These results indicate that specific blockage of Mas increases damage and fibrosis

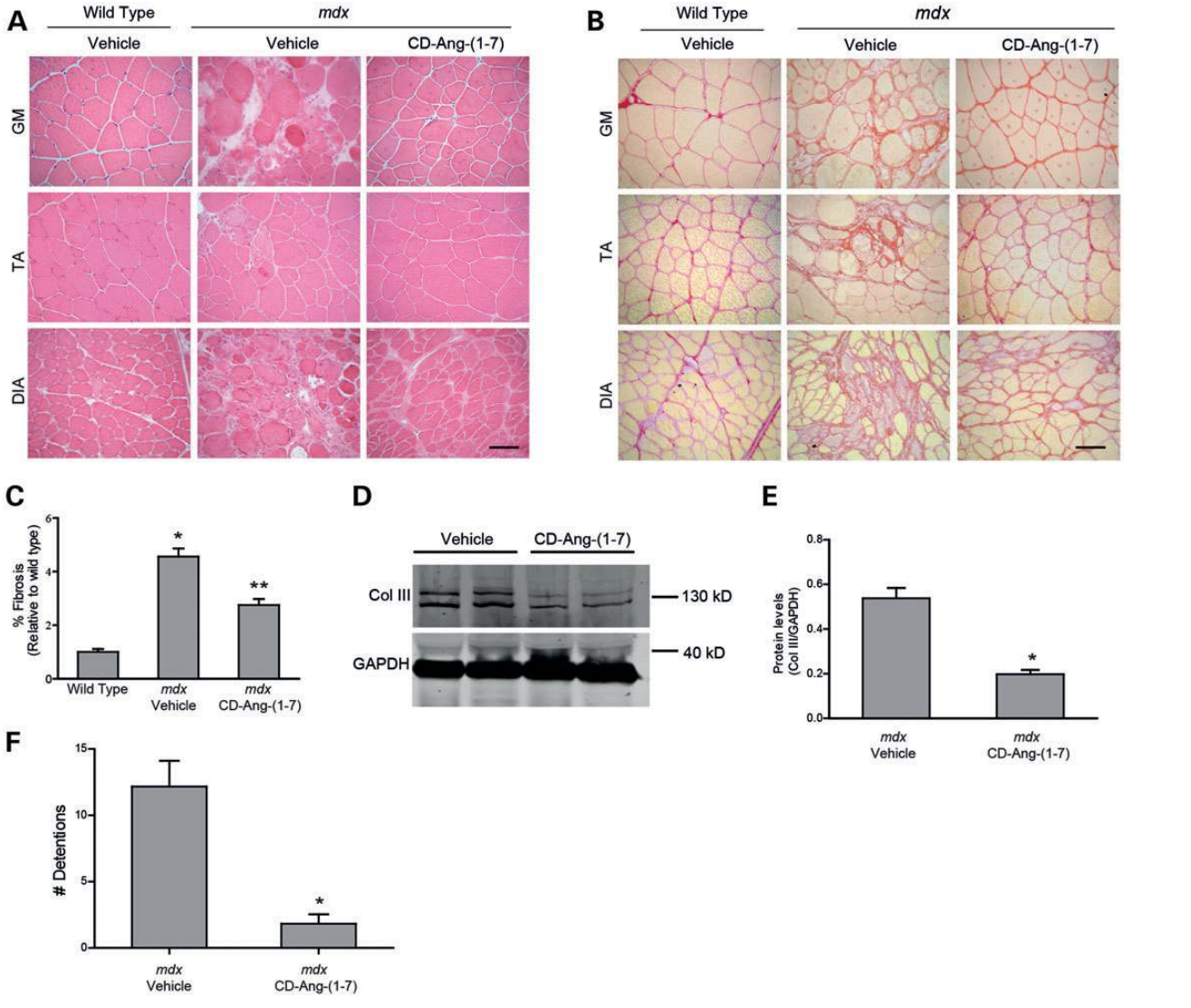

Figure 2. Delivery of Ang-(1-7) included in hydroxypropyl β-cyclodextrin (CD-Ang-(1-7)) present beneficial effects in muscle architecture and muscle function. (**A**) Ang-(1-7) included in hydroxypropyl *β*-cyclodextrin (CD-Ang-(1-7)) was delivered to *mdx* mice via gavage. Architectural improvement was observed by H&E staining in GM, TA and DIA. (**B**) A decrease in the total amount of collagen in GM, TA and DIA were observed in *mdx* mice that received CD-Ang-(1-7) orally. (**C**) Graph shows quantitation of fibrotic area of six fields of GM ($n = 3$ animals per group). One-way ANOVA, $^{*}P < 0.001$ wild-type versus *mdx*, $^{**}P < 0.001$ *mdx* versus *mdx* + CD-Ang-(1-7). (**D**) Western blot analysis of a total GM protein extract showing collagen III reduction after CD-Ang-(1-7) treatment and in untreated *mdx* mice (vehicle), $n = 4$. (**E**) Levels of collagen type III were quantified. *t*-Student $^{*}P < 0.001$ *mdx* versus *mdx* + Ang-(1-7). (**F**) *Mdx* mice treated with CD-Ang-(1-7) performed better in a treadmill test compared with untreated *mdx* mice (vehicle). *t*-Student $^{*}P < 0.001$ *mdx* vehicle versus *mdx* + CD-Ang-(1-7) $n = 4$ animals each group. Scale bar, 50 μm.

and decreases animal running performance and the specific force developed by isolated muscle.

Mdx mice KO for Mas receptor showed deterioration in muscle structure, increased fibrosis and diminished running performance

All the above evidence suggests that the beneficial phenotype observed in the *mdx* skeletal muscle in response to Ang-(1-7) is mediated by inhibition through the Mas receptor. Therefore, we crossed *mdx* with Mas-knockout (Mas-KO) mice (Supplementary Material, Fig. S6A). The *mdx*-Mas-KO mice weighed less than *mdx* mice at 12 weeks of age (Supplementary Material, Table SI). As expected, no Mas receptor transcripts were detected in Mas-KO and *mdx*-Mas-KO GM (Fig. 4A), TA and DIA (Supplementary Material, Fig. S6B and C). The GM histology of Mas-KO mice was indistinguishable from that of the wild-type (Fig. 4B). However, GM and TA from *mdx*-Mas-KO showed a substantial increase in architectural deterioration, inflammation and damaged areas in comparison with *mdx* muscles (Fig. 4B, Supplementary Material, Fig. S6D). The dystrophic GM and TA non-expressing Mas showed an increase in total collagen (Fig. 4C and D) as well as specific collagen type I, III and fibronectin (Fig. 4E, Supplementary Material, Fig. S6E). Western blot analyses indicated an increase in the amount of fibronectin and collagen type III in the *mdx*-Mas-KO mice

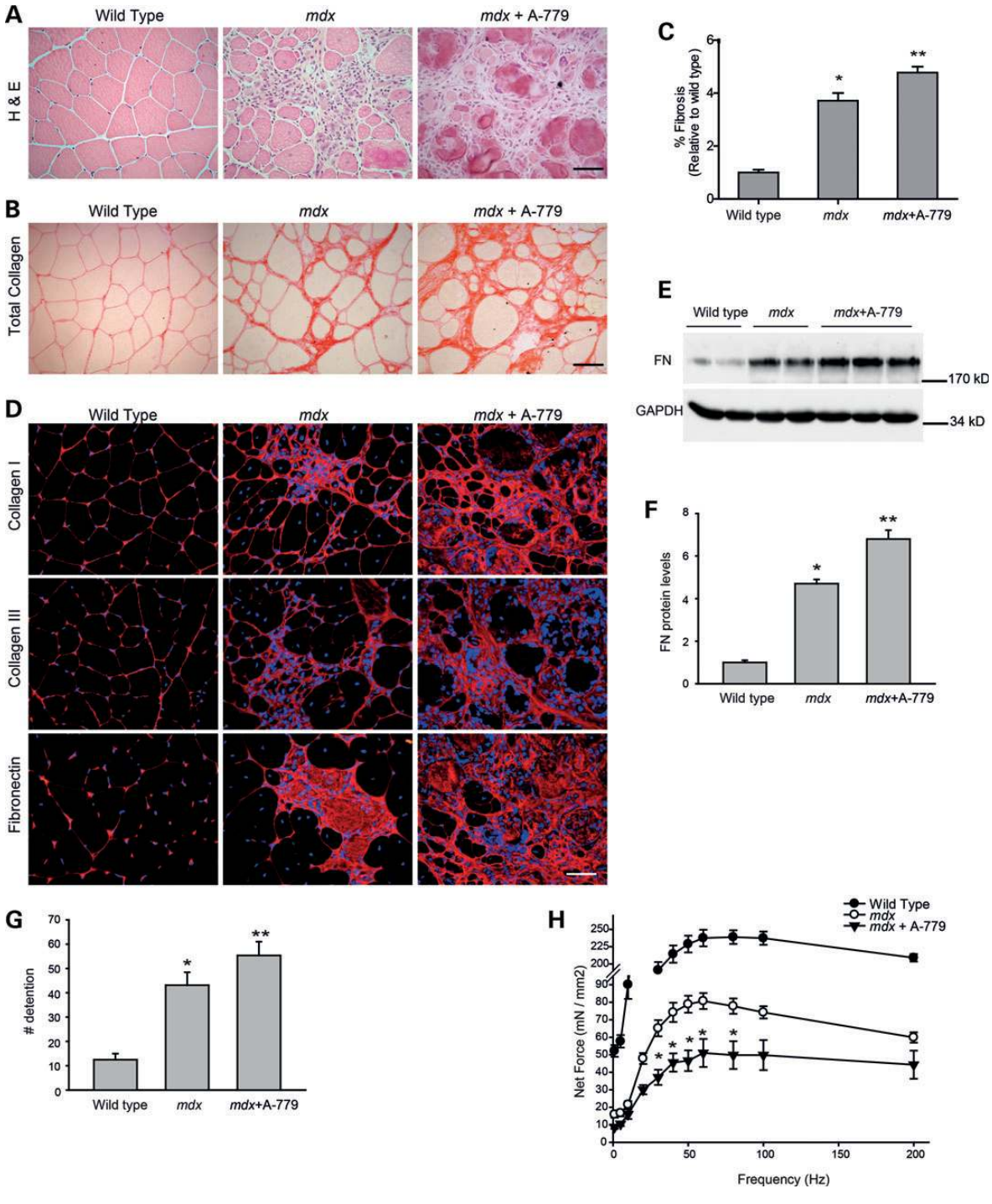

Figure 3. A-779, a potent antagonist of Ang-(1-7), impaired dystrophic muscle histology, increased fibrosis and worsened skeletal muscle force in *mdx*. (**A**) Histological analysis of GM from *mdx* treated with the antagonist A-779. A highly damaged histology is apparent compared with *mdx*. (**B**) Sirius red staining revealed increased accumulation of total collagen in GM from *mdx* infused with the antagonist compared with *mdx* mice. (**C**) Quantitation of fibrosis area of six fields of Sirius red photographs $n = 4$ animals per group. One-way ANOVA, $^{*}P < 0.001$ wild-type versus *mdx*, $^{**}P < 0.05$ *mdx* versus *mdx* + A-779. (**D**) A significant increase in fibrotic proteins (indicated by collagen type I, III and fibronectin) was observed in *mdx* infused with the antagonist in comparison with GM from untreated *mdx* mice. (**E**) Western blot analysis of total proteins from DIA obtained from *mdx* mice infused with A-779 showing an increase in fibronectin levels compared with untreated mice. (**F**) Levels of fibronectin (FN) were quantified based on expression relative to the wild-type. A significant increase in the total amount of FN was observed in DIA from *mdx* mice treated with the antagonist compared with untreated *mdx*. Data correspond to the mean ± SEM (n = 3 animals). One-way ANOVA, $^{*}P < 0.001$ wild-type versus *mdx*, $^{**}P < 0.01$ *mdx* versus *mdx* + A-779. (**G**) *mdx* mice treated with Ang-(1-7) antagonist performed worse in a treadmill test compared with untreated *mdx* mice. Data correspond to the mean ± SEM ($n = 5$ animals). One-way ANOVA, $^{*}P < 0.001$ wild-type versus *mdx*, $^{**}P < 0.01$ *mdx* versus *mdx* + A-779. (H) *In vitro* force–frequency relationship of explanted DIA muscle: isometric net force normalized to muscle CSA (relative tension) versus stimulation frequency (1–200 Hz) was lower in A-779 infused *mdx* mice at frequencies from 30 to 80 Hz than in untreated *mdx* mice. Two-way ANOVA $^{*}P < 0.001$ ($n = 5$ animals). Scale bar, 50 μm.

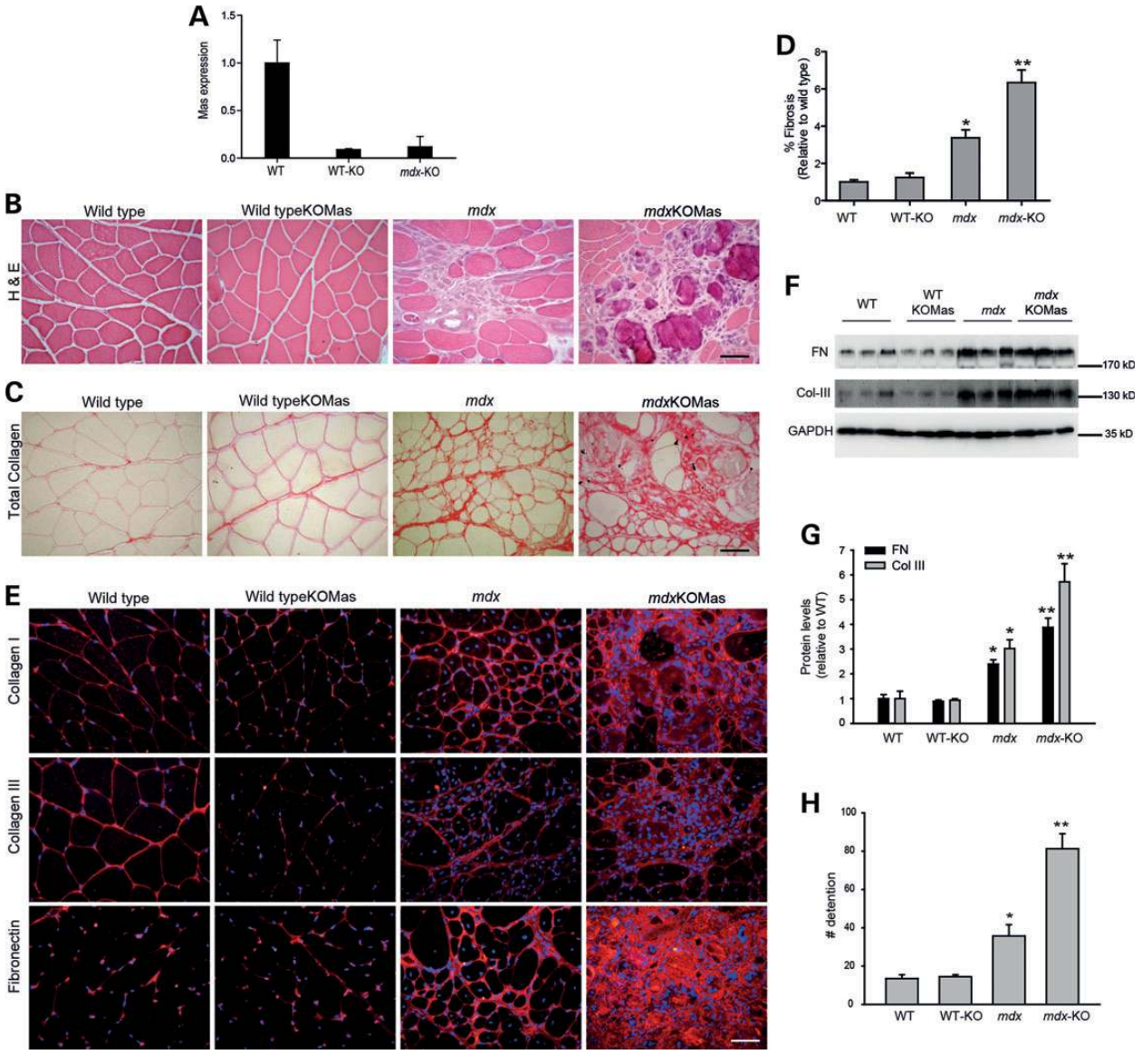

Figure 4. *Mdx* mice KO for Mas receptor showed deterioration in muscle structure, increased fibrosis and diminished running performance. (**A**). As expected, Mas receptor transcripts were not detected in wild-type-Mas-KO and *mdx*-Mas-KO. One-way ANOVA, $^{*}P < 0.05$ wild-type versus *mdx* ($n = 3$ animals). (**B**) GM from *mdx*-Mas-KO shows deterioration in architecture in comparison with GM from *mdx* mice. (**C**) GM from *mdx* mice deficient in Mas receptor shows a significantly important increase in total collagen compared with GM from *mdx* mice, determined by Sirius red staining. (**D**) Quantitation of fibrosis area of six fields of Sirius red photographs $n = 3$ animals per group. One-way ANOVA, $^{*}P < 0.001$ wild-type versus *mdx*, $^{**}P < 0.001$ *mdx* versus *mdx*-Mas-KO. (**E**) Fibrosis (indicated by collagen type I, III and fibronectin staining) was more extensive in GM from *mdx*-Mas-KO mice compared with GM from *mdx* mice. (**F**) Western blot analysis on a total DIA protein extract from wt, wt-Mas-KO, *mdx* and *mdx*-Mas-KO showing increase in fibronectin and collagen in muscle from the *mdx*-Mas-KO compared with *mdx* and wild-type mice. The bands correspond to three different mice DIA muscles in each case. (**G**) Levels of fibronectin (FN) and collagen type III (Col III) were quantified based on expression relative to the wild-type. Data correspond to the mean ± SEM ($n = 3$ animals). One-way ANOVA, $^{*}P < 0.01$ wild-type versus *mdx* $^{**}P < 0.001$ *mdx* versus *mdx*-Mas-KO. (**H**) *mdx*-Mas-KO mice showed poorer performance in a treadmill test compared with *mdx* mice. One-way ANOVA $^{*}P < 0.01$ wild-type versus *mdx* $^{**}P < 0.0001$ *mdx* versus *mdx*-Mas-KO ($n = 5$ animals). Scale bar, 50 μm.

compared with *mdx* DIA (Fig. 4F and G). We evaluated the performance of the *mdx*-Mas-KO mice in a running test. A decline in performance was observed in the *mdx*-Mas-KO compared with *mdx* mice and no differences were observed between wild-type and Mas-KO mice (Fig. 4H).

Ang-(1-7) mediates its effects antagonizing TGF-β signalling pathway involving miR-21 activity

Since it has been shown that TGF-β activity associated with fibrosis is enhanced in *mdx* as well as other muscle disorders (20), we determined the amount of pSmad3 in muscles from *mdx* mice that received Ang-(1-7). A significant decrease in nuclear pSmad3 was observed almost to wild-type levels in the GM (Fig. 5A and B) and TA (Supplementary Material, Fig. S7A and B). In old animals, Ang-(1-7) also reduced TGF-β signalling determined by the nuclear translocation of pSmad3 (Fig. 5C). We also observed a decrease in pSmad3 in muscles of *mdx* treated with CD-Ang-(1-7) compared with muscle sections from *mdx* (Supplementary Material, Fig. S7C and D). Following the observation that Ang-(1-7) diminished

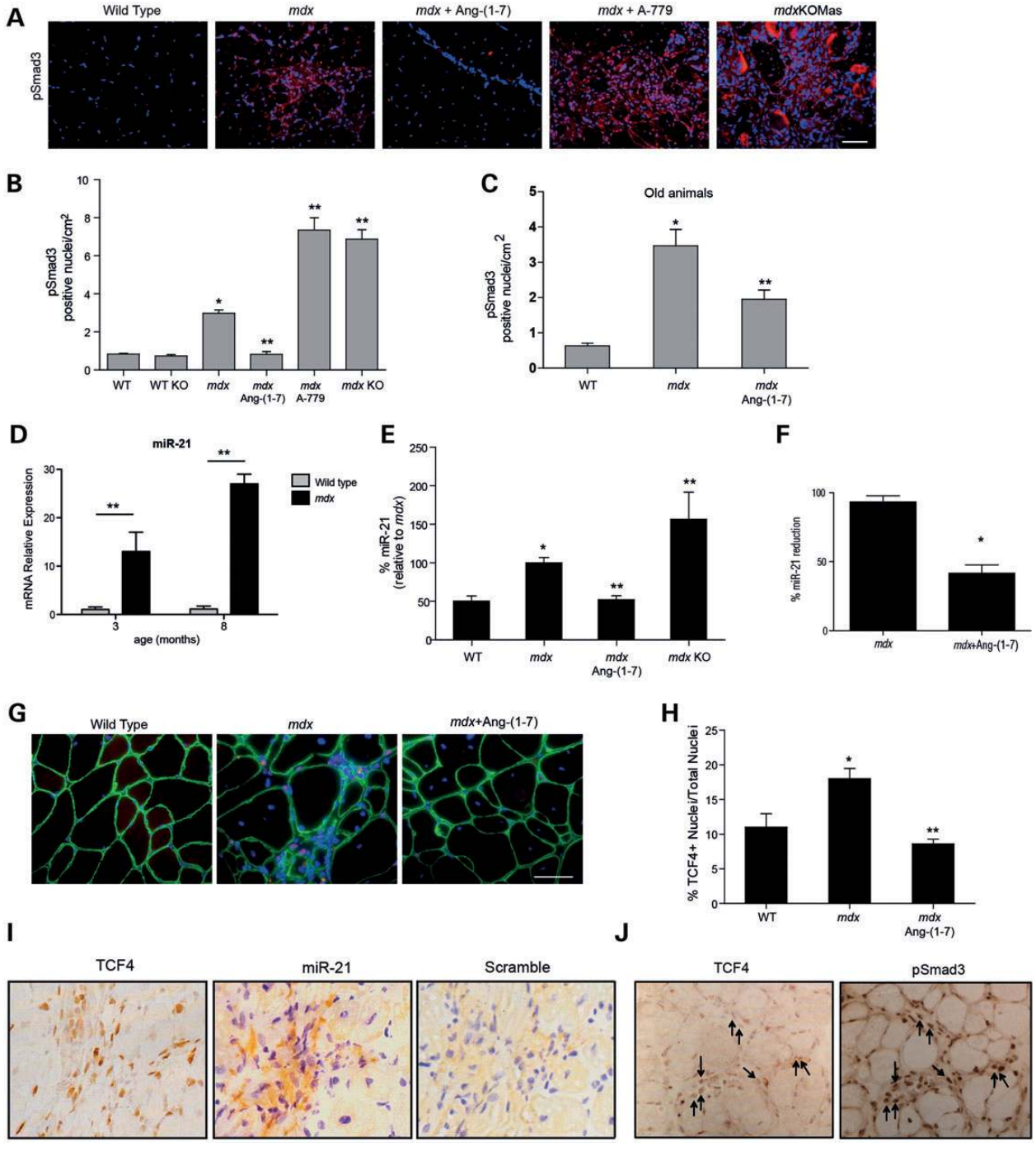

Figure 5. Ang-(1-7) decrease TGF-β mediated signalling, reduces pro-fibrotic microRNA miR-21 and fibroblast population in dystrophic muscle. (**A**) Animals treated with Ang-(1-7) show reduced Smad3 staining of GM and on the contrary is increased in mice treated with A-779 or *mdx*-MasKO. (**B**) Quantitative analysis of pSmad3-positive nuclei in GM from different treatments as in (A). One-way ANOVA, $^{*}P < 0.01$ wild type versus *mdx*, $^{**}P < 0.01$ Ang-(1-7), A-779 or *mdx*-Mas-KO compared with *mdx* mice ($n = 3$ animals). (**C**) The graph shows the decrease in the amount of pSmad3- positive nuclei after Ang-(1-7) infusion in old animals. One-way ANOVA, $^{*}P < 0.001$ wild-type versus *mdx*, $^{**}P < 0.01$ *mdx* mice treated with Ang-(1-7) versus untreated *mdx* mice. (**D**) The expression level of miR-21 was analysed by quantitative PCR comparing wt and *mdx* muscle at 3 and 8 months of age. Data correspond to the mean ± SEM $n = 4$ of each group, $^{**}P < 0.005$. (**E**) miR-21 expression level in GM muscles from *mdx* mice treated or not with Ang-(1-7) and *mdx* MasKO. Data correspond to the mean ± SEM $n = 4$ of each group, $^{*}P < 0.01$, $^{**}P < 0.005$. (**F**) Comparison of miR-21 expression level in GM muscles from old *mdx* mice treated or not with Ang-(1-7). Data correspond to the mean ± SEM $n = 3$ of each group, $^{*}P < 0.01$, $^{**}P < 0.005$. (**G**) Representative TCF4 immunostaining (red) of muscle sections from wild-type, *mdx* and *mdx* mice treated with Ang-(1-7). Laminin immunostaining (green). Nuclei are stained with Hoechst. Bar, 50 μm. (H) Quantification of fibroblasts (identified by TCF4 expression) number per area of GM muscle sections in wild-type, *mdx* and *mdx* mice treated with Ang-(1-7). (**I**) Serial sections of *mdx* GM muscles were subjected to *in situ* hybridization (ISH) with a specific probe for miR-21 expression or a scrambled control probe, and (**J**) immunostaining of GM using antibodies specific for TCF4 and pSmad3. Scale bar, 50 μm.

the nuclear translocation of pSmad3 in *mdx* mice, we assessed the translocation of this TGF-β signalling mediator in response to the infusion of A-779. A significant increase in pSmad3 translocated to the nuclei was observed in GM and DIA (Fig. 5A and B, Supplementary Material, Fig. S7E and F). Finally, TGF-β signalling was also enhanced in the *mdx*-Mas-KO as demonstrated by the increase in pSmad3 translocated to nuclei in GM (Fig. 5A and B) and TA (Supplementary Material, Fig. S7G and H). All these results clearly suggest that Ang-(1-7) through its receptor Mas reduces TGF-β signalling pathway.

Recently, the profibrotic activity of TGF-β in dystrophic muscle was shown to be mediated, at least in part, by a Smad-mediated induction of the microRNA (miR)-21 expression (28). Based on the modulation of TGF-β/Smad signalling in *mdx* mice by Ang-(1-7), we analyzed whether miR-21 could be also modulated by Ang-(1-7) in dystrophic muscle. miR-21 levels increased age-dependently in *mdx* muscle (Fig. 5D); Ang-(1-7) infusion reduced miR-21 expression (Fig. 5E) and on the other hand, muscles from *mdx*-Mas-KO had significantly higher levels of miR-21 expression than *mdx* (Fig. 5E). Notably 2 months of Ang-(1-7) treatment of 8-month-old *mdx* mice reduced miR-21 expression by 55% (Fig. 5F). Next, we evaluated the number of fibroblasts (identified by TCF4 expression) (29), which are the major collagen and ECM producing cells. This cell type was increased in *mdx* muscle compared with wt, and this was reversed by Ang-(1-7) treatment (Fig. 5G and H). Since TCF4-expressing fibroblasts in *mdx* muscle expressed miR-21 (Fig. 5I) and pSmad3 (Fig. 5J), we postulate that Ang-(1-7) might modulate fibroblast function through a Smad/miR-21 axis. These results indicate that infused or orally administered Ang-(1-7) has a beneficial effect on skeletal muscle structure, fibrosis and physiology, involving a decrease in TGF-β Smad signalling, likely mediated by miR-21.

Ang-(1-7) decrease TGF-β mediated signalling in fibroblasts derived from skeletal muscles

Fibroblasts derived from DIA were incubated with TGF-β in the presence or absence of Ang-(1-7). A decrease in the amount of pSmad2 by Ang-(1-7) was observed (Fig. 6A and B). Similarly, the translocation of Smad4 to nuclei was significantly diminished by Ang-(1-7) in fibroblasts derived from DIA (Fig. 6C). We also evaluated if the binding of TGF-β to their transducing receptors was inhibited by Ang-(1-7) in the explanted dystrophic fibroblasts. No changes in the binding were observed (data not shown). These results indicate that Ang-(1-7) inhibits the Smad-dependent signalling mediated by TGF-β.

Reduction of pro-fibrotic microRNA miR-21 by Ang-(1-7) treatment decreases fibroblast population and extracellular matrix production

Since miR-21 induction is mediated by TGF-β, we determined the level of expression of miR-21 in *in vitro* cultured fibroblasts. The fibroblasts up-regulated the expression of miR-21 in response to TGF-β, and this was reversed by Ang-(1-7) treatment (Fig. 7A). Confirming the specificity of the Ang-(1-7) through its receptor Mas, A-779 treatment impaired Ang-(1-7) effect. Of note, the increment of ECM genes, collagen I, fibronectin and collagen III, in fibroblasts following TGF-β stimulation was inhibited by Ang-(1-7) (Fig. 7B), in agreement with the *in vivo* results. Consistent with these findings, ant-miR-21 (antagomir for miR-21) (28) administration also reduced the number of fibroblasts determined by TCF4 + nuclei (Fig. 7C) and ECM production (Fig. 7D) in *mdx* mice.

DISCUSSION

In this article, we show that components of the axis Ang-(1-7)-Mas plays a critical role controlling skeletal muscle damage and fibrosis in DMD. This novel axis counteracts the renin–angiotensin-II axis resulting in opposing actions such as vasodilatation, inhibition of proliferation and anti-fibrotic effects (30–34). Quite remarkable are the results using infusion of the Mas antagonist A-779 (27) and the analysis of skeletal muscles isolated from the *mdx*-Mas-KO mice. An important increase in tissue damage, accompanied of fibrosis, increase in TGF-β signalling and a significant decrease in isolated skeletal muscle force and in performance in a running test were observed. These results suggest that endogenous Ang-(1-7) is acting in the skeletal muscle maintaining a more permissive phenotype in the *mdx* mice. We have preliminary evidence indicating that ACE2 and Mas are expressed in skeletal muscle; these observations open the possibility that the generation and the action of the hepta-peptide occurs in the tissue itself. Further experiments of tissue-specific gain and loss of function for these two members of the axis ACE2-Ang-(1-7)-Mas are required. The decrease in fibrosis observed in the *mdx* animals treated with Ang-(1-7) was associated with better preservation of muscular functionality, as evidenced by skeletal muscle force analyses and functional tests of exercise endurance.

Expression of myogenic factors is essential but not sufficient for successful skeletal muscle formation (35). It has been shown that a properly organized ECM is an absolute requirement for skeletal muscle formation and maintenance (36). Fibrosis might destabilize the interactions between skeletal muscle fibre receptors, such as integrins (37,38) and membrane-bound heparan sulphate proteoglycans (39–42), and the surrounding basal lamina. Therefore, in mice with an increased Ang-(1-7), and thereby less ECM accumulation around individual fibres, better communication between muscle cells and the basal lamina might also have contributed to reduction of the dystrophic phenotype.

It has been shown that abnormal TGF-β signalling is linked to several forms of muscular dystrophy including DMD, Becker and Emery-Dreifuss (43–46). TGF-β signalling is involved in the fibrotic process, as well as in several myopathies. Inhibiting TGF-β can reduce fibrosis and improve regeneration in several genetic forms of myopathy, including dystrophin-negative DMD and Marfan syndrome (20,46–48). The inhibition in TGF-β signalling observed using ARB attenuates TGF-β-induced failure of muscle regeneration (20,21,47). It has been hypothesized that the increase in ACE2 will produce more Ang-(1-7) with the concomitant decrease in the amount of angiotensin II (49). The attractive observation that the ARB Losartan reduces the fibrotic effect is consistent with an increase of the concentration of angiotensin II, and therefore more substrate for ACE2 should be available producing more Ang-(1-7) which could interact with Mas and produce the beneficial effects on the dystrophic skeletal muscle, as the one described in this article. Further experiments, using Losartan

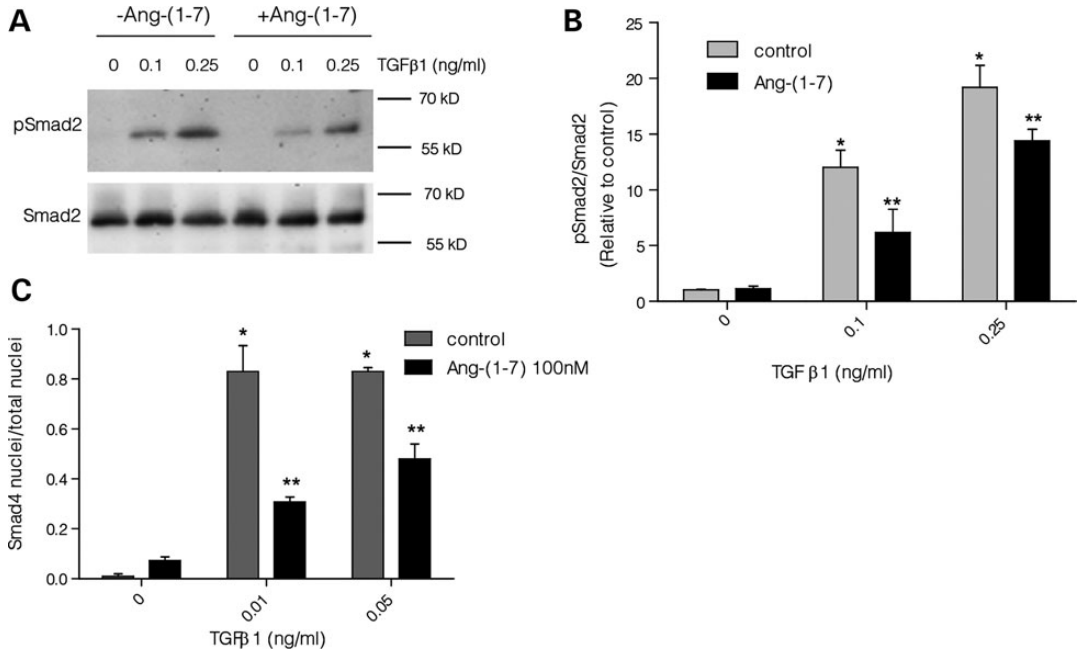

Figure 6. Ang-(1-7) decrease TGF-β mediated signalling in fibroblasts derived from skeletal muscles. (**A**) Fibroblasts derived from DIA were incubated with TGF-β in the presence or absence of Ang-(1-7) 100 nM. Western blot analysis shows a reduction of pSmad2 in fibroblast treated with Ang-(1-7). (**B**) Levels of pSmad2 were quantified based on expression relative to control. Data correspond to the mean ± SEM ($n = 3$). One-way ANOVA, $^{*}P < 0.01$ control versus TGF-β, $^{**}P < 0.001$ TGF-β versus TGF-β + Ang-(1-7). (**C**) Quantitation of Smad4 positive nuclei assessed by immunostaining of fibroblast derived from DIA muscle sections from wild-type mice treated with Ang-(1-7) in the presence of absence of TGF-β. Data are mean ± SEM. One way ANOVA, $^{*}P < 0.001$ control versus TGF-β, $^{**}P < 0.001$ TGF-β versus TGF-β + Ang-(1-7) $n = 3$.

in the presence of an antagonist of Mas or Losartan infusion in *mdx*-Mas-KO should clarify this appealing re-interpretation of the current data.

Interestingly, we observed an important decrease, *in vivo* and *in vitro* in the amount of pSmad2/3 after treatment with Ang-(1-7). This decrease is not a consequence of a competition of Ang-(1-7) for the binding of TGF-β to the transducing receptors (data not shown). We have previously demonstrated that TGF-β decrease the amount of Smad7 (28), an inhibitory protein of pSmad2/3 (19). Furthermore, we have experimental evidence in skeletal muscle-derived fibroblasts that indicates that Ang-(1-7) avoid this decrease and is through Mas. In dystrophic muscle, we observed that Smad7 expression is diminished and infusion of Ang-(1-7) increase its expression (data not shown). Further experiments require to be designed to prove that this is one(s) of the mechanism responsible of the decrease in pSmad2/3 in response to Ang-(1-7).

We have shown before that miR-21 expression appears dysregulated in dystrophic muscle which is enhanced in response to TGF-β (28). We determined that Ang-(1-7) reduced the amount of pro-fibrotic miR-21 in isolated skeletal muscle fibroblasts and *mdx* skeletal muscle and was significantly increased in skeletal muscle isolated from *mdx*-Mas-KO. In fibroblasts positive for TCF4 co-localization of miR-21 and pSmad3 was observed, suggesting that this cell type is responding to TGF-β. A higher increase in miR-21 together with a reduction by Ang-(1-7) was also observed in skeletal muscle from old mice, indicating that the regulation of the fibrotic phenotype via miR-21 is a general phenomenon in *mdx* skeletal muscles. Thus, miR-21 seems to be a direct target for TGF-β signalling downstream pSmad3. Interestingly, *mdx* mice treated with anti-miR-21 showed a decrease in the number of TCF4-positive fibroblasts and in the expression of fibronectin and collagen type I. The role of miRs in regulation of TGF-β-mediated signalling in *mdx* skeletal muscle has been reported previously. TGF-β regulates negatively the expression of the antifibrotic miR-29 promoting the formation of myofibroblasts (50), and the degree of damage observed in dystrophic phenotype is inverse to the amount of miR-29 (51). It would be interesting to evaluate whether the expression of miR-29 increases in skeletal muscles of *mdx* treated with Ang-(1-7).

Fibrosis in dystrophic mice increase with age (52), the improvement in the phenotype and skeletal muscle function of *mdx* mice treated with Ang-(1-7) was observed in young and old mice, opening the possibility that this compound could be used as a therapeutic agent to treat muscular dystrophies. In this context, we also observed an important improvement in the phenotype of the *mdx* skeletal muscles, together with a decrease in fibrosis and a significant improvement in the exercise test when Ang-(1-7) was delivered by gavage to *mdx* mice. This was obtained by associating Ang-(1-7) to hydroxypropyl β-cyclodextrin (CD-Ang-(1-7)) (26). This associated compound that partially encapsulates Ang-(1-7) has the potential to be a feasible formulation for oral administration of Ang-(1-7), which can be used for improvement of skeletal muscular dystrophies.

Ang-(1-7) might be used to improve quality of life and delay death in individuals with DMD. However, this drug should be investigated in further pre-clinical trials. Extrapolation of studies in (small) mice to clinical treatment of (large) humans can be very difficult. The use of Ang-(1-7) as shown in this

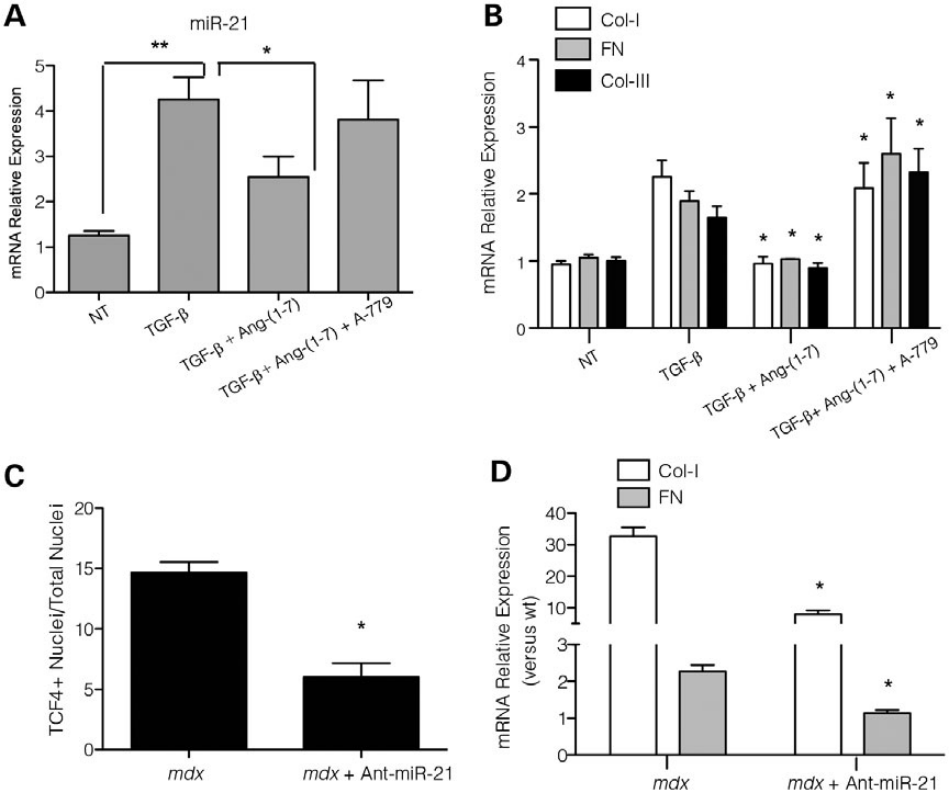

Figure 7. Reduction of pro-fibrotic microRNA miR-21 by Ang-(1-7) treatment decreases fibroblast population and extracellular matrix production. (**A**) Wild-type fibroblasts were stimulated or not with TGF-β, in the absence or presence of Ang-(1-7), or Ang-(1-7) and the inhibitor of Mas receptor A-779, and miR-21 expression was analyzed by quantitative PCR (**$P < 0.005$, *$P < 0.05$; means ± SEM; $n = 4$ for each group). (**B**) Wild-type fibroblasts, stimulated as in (A), were analyzed for Col-I, FN and Col-III expression (*$P < 0.05$; means ± SEM; $n = 4$ for each group). (**C**) Quantification of fibroblasts from muscles of *mdx* mice, and *mdx* mice treated with AntmiR-21, after TCF4 immunohistochemistry. Data obtained were expressed as a fold increase in *mdx* versus wild-type muscles (*$P < 0.01$; means ± SEM; $n = 4$ for each group). (**D**) Muscles of *mdx* mice, treated or not with Ant-miR-21, were analyzed for Col I and FN expression by quantitative PCR (*$P < 0.05$; means ± SEM; $n = 4$ for each group).

article is promissory. Ang-(1-7) exhibits high selectivity and specificity for its receptor and can therefore be used as an agonist. However, Ang-(1-7) is a peptide and thus has a short plasma half-life and is rapidly degraded in the gastrointestinal tract when given orally. Thus, attempts to make Mas stimulation suitable for clinical use mainly concentrate on finding orally active formulations/derivatives of Ang-(1-7) or at least increasing its plasma half-life; in this context, various studies with different Ang-(1-7) formulations are being tested in different models of diseases such as hypertension, pulmonary, renal and cardiac fibrosis and shown beneficial effects (34). In this regard, we have shown in this study that treatment with CD-Ang-(1-7) at least in the *mdx* mice model has the same effects than Ang-(1-7) via systemic infusion giving the hope for future therapeutics options with this oral formulation in the field of muscular disorders.

MATERIALS AND METHODS

Mice

Wild-type, *mdx* (C57BL/10ScSn) (5), wild-type Mas-KO (C57B16) (53) and *mdx*-Mas-KO (12 weeks old) male mice were used. Experimental exercise was achieved by running the mice in a treadmill three times a week, for 30 min on each occasion, at 12 m/min for 2 months starting at 12 weeks of age (54). Increase in skeletal muscle damage and fibrosis is shown in Supplementary Material, Figure S2A–C. Experiments were also performed in 8-month-old control and *mdx* mice treated for 2 months, but without exercising, data were collected at 10 month old. Increase in damage and fibrosis is shown in Supplementary Material, Figure S2D–F. All mouse protocols were approved by the Animal Care and Use Committee of the Catholic University of Chile and Universidade Federal Minas Gerais, Brazil. At the end of the experiment, animals were anesthetized and sacrificed by cervical dislocation; GM, TA and DIA were dissected and removed. Tissues were rapidly frozen and stored at −80°C until processing or use immediately for electrophysiological measurement (55,56).

Angiotensin-(1-7) treatment

Wild-type, *mdx* mice were started on treatment at 12 weeks of age using an osmotic minipump (Alzet, Durect Co., 1004 model) s.c. at a pumping dose of Ang-(1-7) (100 ng/kg min) for 8 weeks. In addition, Ang-(1-7) included in hydroxypropyl β-cyclodextrin (HPβCD) (CD-Ang-(1-7) (50 μg/kg) (26) was administered daily to mice by oral gavage for 4 weeks. Fibrosis and running performance were evaluated at the end of each experiment.

Antagonism of Mas receptor with A-779 treatment

Twelve-week-old male *mdx* mice were started on treatment with a potent antagonist of the Mas receptor, A-779 [D Ala-Angiotensin-(1-7), Phoenix Pharmaceuticals, USA] via osmotic minipumps at a rate of (100 ng/kg min) for 2 months and tissue was collected at this time.

TGF-β intramuscular injection

Twelve-week-old male wild-type mice were used for TGF-β1 intramuscular injection. Mice were anesthetized with isofluorane, and 20 ng of recombinant human TGF-β1 (R&D systems), dissolved in 50 ml of saline (0.9% NaCl), were directly injected into the TA muscle, using an insulin syringe. The contralateral TA was injected with 50 μl saline as control (22,57), and 24 h later, both TA were collected for western blot analysis.

Ant-miR-21 treatment

For miR treatment *in vivo*, 5 μg of ant-miR-21 was administered in dystrophic muscle as described (28).

RNA isolation, reverse transcription and quantitative real-time PCR

Total RNA was isolated from GM, TA and DIA using Trizol (Invitrogen, USA) according to the manufacturer's instructions. Total RNA (2 μg) was reverse-transcribed to cDNA using random hexamers and Superscript reverse transcriptase (Invitrogen). TaqMan quantitative real-time PCR reactions were performed in duplicate on a Stratagene MX 3005 Thermocycler (Agilent Technology), using predesigned primer sets for mouse Mas and the housekeeping gene GAPDH (TaqMan Assays-on-Demand, Applied Biosystems, USA). mRNA expression was quantified using the comparative dCt method (2-ΔΔCT), using GAPDH as the reference gene. mRNA levels were expressed relative to the mean expression of the wild-type mice.

Immunoblot analysis

For immunoblot analyses, DIA or GM muscles were homogenized in 10 volumes of buffer Tris-EDTA pH 7.4 with 1 mM PMSF, after which one volume of buffer containing 2% glycerol, 4% SDS and 0.125 M Tris pH 6.8 were added to the homogenates. Aliquots were subjected to SDS gel electrophoresis in 10% polyacrylamide gels, electrophoretically transferred onto PVDF membranes (Millipore, USA) and probed with specific antibodies against fibronectin, tubulin (Sigma-Aldrich, USA), collagen III (Rockland, USA) and GAPDH (Chemicon, USA). All immunoreactions were visualized by enhanced chemiluminescence (Pierce, USA) (56).

Immunofluorescence microscopy

For muscle immunofluorescence, cryosections (7 μm) were fixed in 4% paraformaldehyde, blocked for 1 h in 10% goat serum in PBS and incubated for 1 h at room temperature with anti-fibronectin (Sigma, USA), anti-collagen III (Rokland), anti-collagen I (Abcam, USA), anti-phosphoSmad3 (Invitrogen) (55,56) and anti-TCF4 (Cell Signaling). The corresponding Alexa Fluor 568-conjugated anti-IgG was used as secondary antibodies. For nuclear staining, sections were incubated with 1 μg/ml Hoechst 33258 in PBS for 10 min.

phosphoSmad3 quantification

We counted the number of positive nuclei for pSmad3 staining using the ImageJ v1.43u 'cell counter' plugin, from 10 different frames for each analysed muscle at ×40 magnification. The data obtained were corrected for total area.

TCF4-positive nuclei quantification

We counted the number of positive nuclei for TCF4 staining using Photoshop with the count tool, from 20 different frames for each analysed muscle at ×60 magnification. The data obtained were corrected for total nuclei.

Skeletal muscle histology and Sirius red staining

GM, DIA and TA cryosections were placed onto glass slides. Haematoxylin and eosin staining was performed to assess muscle architecture and histology. Total collagen content was detected by staining with 1% Sirius red in picric acid (55,56). For Sirius red quantification ImageJ software was used, calculating percentage of red stained area (% of fibrosis) and the data are expressed relative to wild-type which resulted in 3.8 ± 0.4% of fibrosis.

In situ hybridization

In situ hybridization was performed in cryosections from GM muscles using antisense locked nucleic acid (LNA)-modified oligonucleotides (58), following the procedure previously described (28). LNA/DNA oligonucleotides contained LNAs at eight consecutive centrally located bases and had the following sequences: LNA-miR-21 5′-TCAACATCAGTCTGATAAGCTA-3′ and LNA-scrambled 5′-CATTAATGTCGGACAACTCAAT-3′.

Contractile properties

After the indicated days of treatment, the mice were sacrificed and the DIA rapidly excised into a dish containing oxygenated Krebs-Ringer solution. Muscle strength was determined as described previously (55,56). The optimum muscle length (Lo) and stimulation voltage were determined from micromanipulations of muscle length to produce the maximum isometric twitch force. Maximum isometric specific tetanic force was determined from the plateau of the curve of the relationship between specific isometric force (mN/mm^2) with a stimulation frequency (Hz) ranging from 1 to 200 Hz for 450 ms, with 2 min of rest between stimuli. Muscle mass and Lo were used to calculate the specific net force (force normalized per total muscle fibre cross-sectional area (CSA), mN/mm^2].

Running test

Wild-type, wild-type Mas-KO, *mdx* and *mdx*-Mas-KO mice were subjected to a running test for 5 min at 15 m/min in a treadmill. The number of times that mice were slow down to the first third of the moving platform was counted and was defined as number of detentions.

Cell culture and isolation of primary cells

Primary fibroblasts were isolated from mouse muscle as previously described (28). When indicated, cells were stimulated for 24 h with 10 ng/ml recombinant active TGF-β1 (R&D Systems), in the presence of 1 nM Ang-(1-7) or 1 nM Ang-(1-7) and 10 μM A-779.

Statistics

The statistical significance of the differences between the means of the experimental groups was evaluated using one-way ANOVA with a *post hoc* Bonferroni multiple comparison test (Graph Pad Prism 5.00). A difference was considered statistically significant at $P < 0.05$. Student's *t*-test was performed when only two experimental groups were compared. A two-way ANOVA was performed for the *in vitro* strength test in which two parameters (frequency and strength) were analyzed for each data group.

SUPPLEMENTARY MATERIAL

Supplementary Material is available at *HMG* online.

ACKNOWLEDGEMENTS

We would like to thank Victor Troncoso, Ana Vasquez, Lina Correa, José Roberto Sezé and Marilene Oliveira, for technical support.

Conflict of Interest statement. None declared.

FUNDING

This study was supported by research grants from CARE PFB12/2007, FONDECYT 1110426, CONICYT AT-2410061, Fundación Chilena para Biología Celular, Proyecto MF-100, MDA (E.B.), MDA (P.M.-C.), SAF2012-38547, PLE2009-0124 Optistem/Endostem and AFM.

REFERENCES

1. Matsumura, K. and Campbell, K.P. (1994) Dystrophin-glycoprotein complex: its role in the molecular pathogenesis of muscular dystrophies. *Muscle Nerve*, **17**, 2–15.
2. Blake, D.J., Weir, A., Newey, S.E. and Davies, K.E. (2002) Function and genetics of dystrophin and dystrophin-related proteins in muscle. *Physiol. Rev.*, **82**, 291–329.
3. Mann, C.J., Perdiguero, E., Kharraz, Y., Aguilar, S., Pessina, P., Serrano, A.L. and Munoz-Canoves, P. (2011) Aberrant repair and fibrosis development in skeletal muscle. *Skeletal Muscle*, **1**, 21.
4. Serrano, A.L. and Munoz-Canoves, P. (2010) Regulation and dysregulation of fibrosis in skeletal muscle. *Exp. Cell Res.*, **316**, 3050–3058.
5. Caceres, S., Cuellar, C., Casar, J.C., Garrido, J., Schaefer, L., Kresse, H. and Brandan, E. (2000) Synthesis of proteoglycans is augmented in dystrophic mdx mouse skeletal muscle. *Eur. J. Cell Biol.*, **79**, 173–181.
6. Wynn, T.A. (2008) Cellular and molecular mechanisms of fibrosis. *J. Pathol.*, **214**, 199–210.
7. Wynn, T.A. (2007) Common and unique mechanisms regulate fibrosis in various fibroproliferative diseases. *J. Clin. Invest.*, **117**, 524–529.
8. Marangoni, R.A., Carmona, A.K., Passaglia, R.C., Nigro, D., Fortes, Z.B. and de Carvalho, M.H. (2006) Role of the kallikrein-kinin system in Ang-(1-7)-induced vasodilation in mesenteric arterioles of Wistar rats studied in vivo-in situ. *Peptides*, **27**, 1770–1775.
9. Ferrario, C.M., Trask, A.J. and Jessup, J.A. (2005) Advances in biochemical and functional roles of angiotensin-converting enzyme 2 and angiotensin-(1-7) in regulation of cardiovascular function. *Am. J. Physiol. Heart Circ. Physiol.*, **289**, H2281–H2290.
10. Tallant, E.A., Ferrario, C.M. and Gallagher, P.E. (2005) Angiotensin-(1-7) inhibits growth of cardiac myocytes through activation of the mas receptor. *Am. J. Physiol. Heart Cir. Physiol.*, **289**, H1560–H1566.
11. Iwata, M., Cowling, R.T., Gurantz, D., Moore, C., Zhang, S., Yuan, J.X. and Greenberg, B.H. (2005) Angiotensin-(1-7) binds to specific receptors on cardiac fibroblasts to initiate antifibrotic and antitrophic effects. *Am. J. Physiol. Heart Circ. Physiol.*, **289**, H2356–H2363.
12. Grobe, J.L., Mecca, A.P., Lingis, M., Shenoy, V., Bolton, T.A., Machado, J.M., Speth, R.C., Raizada, M.K. and Katovich, M.J. (2007) Prevention of angiotensin II-induced cardiac remodeling by angiotensin-(1-7). *Am. J. Physiol. Heart Cir. Physiol.*, **292**, H736–H742.
13. Benter, I.F., Ferrario, C.M., Morris, M. and Diz, D.I. (1995) Antihypertensive actions of angiotensin-(1-7) in spontaneously hypertensive rats. *Am. J. Physiol.*, **269**, H313–H319.
14. Ferreira, A.J., Santos, R.A. and Almeida, A.P. (2001) Angiotensin-(1-7): cardioprotective effect in myocardial ischemia/reperfusion. *Hypertension*, **38**, 665–668.
15. Santos, R.A., Simoes e Silva, A.C., Maric, C., Silva, D.M., Machado, R.P., de Buhr, I., Heringer-Walther, S., Pinheiro, S.V., Lopes, M.T., Bader, M. *et al.* (2003) Angiotensin-(1-7) is an endogenous ligand for the G protein-coupled receptor Mas. *Proc. Natl Acad. Sci. USA*, **100**, 8258–8263.
16. Warner, F.J., Lubel, J.S., McCaughan, G.W. and Angus, P.W. (2007) Liver fibrosis: a balance of ACEs? *Clin. Sci. (Lond.)*, **113**, 109–118.
17. Prud'homme, G.J. (2007) Pathobiology of transforming growth factor beta in cancer, fibrosis and immunologic disease, and therapeutic considerations. *Lab. Invest.*, **87**, 1077–1091.
18. Vial, C., Zuniga, L.M., Cabello-Verrugio, C., Canon, P., Fadic, R. and Brandan, E. (2008) Skeletal muscle cells express the profibrotic cytokine connective tissue growth factor (CTGF/CCN2), which induces their dedifferentiation. *J. Cell. Physiol.* **215**, 410–421.
19. Massague, J. (2000) How cells read TGF-beta signals. *Nat. Rev. Mol. Cell. Biol.*, **1**, 169–178.
20. Cohn, R.D., van Erp, C., Habashi, J.P., Soleimani, A.A., Klein, E.C., Lisi, M.T., Gamradt, M., ap Rhys, C.M., Holm, T.M., Loeys, B.L. *et al.* (2007) Angiotensin II type 1 receptor blockade attenuates TGF-beta-induced failure of muscle regeneration in multiple myopathic states. *Nat. Med.*, **13**, 204–210.
21. Burks, T.N., Andres-Mateos, E., Marx, R., Mejias, R., Van Erp, C., Simmers, J.L., Walston, J.D., Ward, C.W. and Cohn, R.D. (2011) Losartan restores skeletal muscle remodeling and protects against disuse atrophy in sarcopenia. *Sci. Trans. Med.*, **3**, 82ra37.
22. Cabello-Verrugio, C., Santander, C., Cofre, C., Acuna, M.J., Melo, F. and Brandan, E. (2012) The internal region leucine-rich repeat 6 of decorin interacts with low density lipoprotein receptor-related protein-1, modulates transforming growth factor (TGF)-beta-dependent signaling, and inhibits TGF-beta-dependent fibrotic response in skeletal muscles. *J. Biol. Chem.*, **287**, 6773–6787.
23. Pierno, S., Nico, B., Burdi, R., Liantonio, A., Didonna, M.P., Cippone, V., Fraysse, B., Rolland, J.F., Mangieri, D., Andreetta, F. *et al.* (2007) Role of tumour necrosis factor alpha, but not of cyclo-oxygenase-2-derived eicosanoids, on functional and morphological indices of dystrophic progression in mdx mice: a pharmacological approach. *Neuropathol. Appl. Neurobiol.*, **33**, 344–359.
24. Beggs, M.L., Nagarajan, R., Taylor-Jones, J.M., Nolen, G., Macnicol, M. and Peterson, C.A. (2004) Alterations in the TGFbeta signaling pathway in myogenic progenitors with age. *Aging cell.*, **3**, 353–361.
25. Pastoret, C. and Sebille, A. (1995) Mdx mice show progressive weakness and muscle deterioration with age. *J. Neurol. Sci.*, **129**, 97–105.

26. Marques, F.D., Ferreira, A.J., Sinisterra, R.D., Jacoby, B.A., Sousa, F.B., Caliari, M.V., Silva, G.A., Melo, M.B., Nadu, A.P., Souza, L.E. *et al.* (2011) An oral formulation of angiotensin-(1-7) produces cardioprotective effects in infarcted and isoproterenol-treated rats. *Hypertension*, **57**, 477–483.
27. Santos, R.A., Campagnole-Santos, M.J., Baracho, N.C., Fontes, M.A., Silva, L.C., Neves, L.A., Oliveira, D.R., Caligiorne, S.M., Rodrigues, A.R., Gropen Junior, C. *et al.* (1994) Characterization of a new angiotensin antagonist selective for angiotensin-(1-7): evidence that the actions of angiotensin-(1-7) are mediated by specific angiotensin receptors. *Brain Res. Bull.*, **35**, 293–298.
28. Ardite, E., Perdiguero, E., Vidal, B., Gutarra, S., Serrano, A.L. and Munoz-Canoves, P. (2012) PAI-1-regulated miR-21 defines a novel age-associated fibrogenic pathway in muscular dystrophy. *J. Cell Biol.*, **196**, 163–175.
29. Mathew, S.J., Hansen, J.M., Merrell, A.J., Murphy, M.M., Lawson, J.A., Hutcheson, D.A., Hansen, M.S., Angus-Hill, M. and Kardon, G. (2011) Connective tissue fibroblasts and Tcf4 regulate myogenesis. *Development*, **138**, 371–384.
30. Pereira, R.M., dos Santos, R.A., da Costa Dias, F.L., Teixeira, M.M. and Simoes e Silva, A.C. (2009) Renin-angiotensin system in the pathogenesis of liver fibrosis. *World J. Gastroenterol.*, **15**, 2579–2586.
31. Iwai, M. and Horiuchi, M. (2009) Devil and angel in the renin-angiotensin system: ACE-angiotensin II-AT1 receptor axis vs. ACE2-angiotensin-(1-7)-Mas receptor axis. *Hypertens. Res.*, **32**, 533–536.
32. Santos, R.A., Ferreira, A.J., Verano-Braga, T. and Bader, M. (2013) Angiotensin-converting enzyme 2, angiotensin-(1-7) and Mas: new players of the renin-angiotensin system. *J. Endocrinol.*, **216**, R1–R17.
33. Fraga-Silva, R.A., Da Silva, D.G., Montecucco, F., Mach, F., Stergiopulos, N., da Silva, R.F. and Santos, R.A. (2012) The angiotensin-converting enzyme 2/angiotensin-(1-7)/Mas receptor axis: a potential target for treating thrombotic diseases. *Thromb. Haemostasis.*, **108**, 1089–1096.
34. Bader, M., Santos, R.A., Unger, T. and Steckelings, U.M. (2012) New therapeutic pathways in the RAS. *J. Ren. Ang. Aldost. Syst.*, **13**, 505–508.
35. Melo, F., Carey, D.J. and Brandan, E. (1996) Extracellular matrix is required for skeletal muscle differentiation but not myogenin expression. *J. Cell Biochem.*, **62**, 227–239.
36. Osses, N. and Brandan, E. (2002) ECM is required for skeletal muscle differentiation independently of muscle regulatory factor expression. *Am. J. Physiol. Cell Physiol.*, **282**, C383–C394.
37. Fadic, R. (2005) Cell surface and gene expression regulation molecules in dystrophinopathy: mdx vs. Duchenne. *Biol. Res.*, **38**, 375–380.
38. Cohn, R.D., Mayer, U., Saher, G., Herrmann, R., van der Flier, A., Sonnenberg, A., Sorokin, L. and Voit, T. (1999) Secondary reduction of alpha7B integrin in laminin alpha2 deficient congenital muscular dystrophy supports an additional transmembrane link in skeletal muscle. *J. Neurol. Sci.*, **163**, 140–152.
39. Cornelison, D., Filla, M., Stanley, H., Rapraeger, A. and Olwin, B. (2001) Syndecan-3 and syndecan-4 specifically mark skeletal muscle satellite cells and are implicated in satellite cell maintenance and muscle regeneration. *Dev. Biol.*, **239**, 79–94.
40. Cornelison, D.D., Wilcox-Adelman, S.A., Goetinck, P.F., Rauvala, H., Rapraeger, A.C. and Olwin, B.B. (2004) Essential and separable roles for Syndecan-3 and Syndecan-4 in skeletal muscle development and regeneration. *Genes Dev.*, **18**, 2231–2236.
41. Casar, J.C., Cabello-Verrugio, C., Olguin, H., Aldunate, R., Inestrosa, N.C. and Brandan, E. (2004) Heparan sulfate proteoglycans are increased during skeletal muscle regeneration: requirement of syndecan-3 for successful fiber formation. *J. Cell Sci.*, **117**, 73–84.
42. Gutierrez, J. and Brandan, E. (2010) A novel mechanism of sequestering fibroblast growth factor 2 by glypican in lipid rafts, allowing skeletal muscle differentiation. *Mol. Cell. Biol.*, **30**, 1634–1649.
43. Burks, T.N. and Cohn, R.D. (2011) Role of TGF-beta signaling in inherited and acquired myopathies. *Skeletal Muscle*, **1**, 19.
44. Kollias, H.D. and McDermott, J.C. (2008) Transforming growth factor-beta and myostatin signaling in skeletal muscle. *J. Appl. Physiol.*, **104**, 579–587.
45. Chen, Y.W., Nagaraju, K., Bakay, M., McIntyre, O., Rawat, R., Shi, R. and Hoffman, E.P. (2005) Early onset of inflammation and later involvement of TGFbeta in Duchenne muscular dystrophy. *Neurology*, **65**, 826–834.
46. Zhou, L. and Lu, H. (2010) Targeting fibrosis in Duchenne muscular dystrophy. *J. Neuropathol. Exp. Neurol.*, **69**, 771–776.
47. Elbaz, M., Yanay, N., Aga-Mizrachi, S., Brunschwig, Z., Kassis, I., Ettinger, K., Barak, V. and Nevo, Y. (2012) Losartan, a therapeutic candidate in congenital muscular dystrophy: studies in the dy(2J) /dy(2J) mouse. *Ann. Neurol.*, **71**, 699–708.
48. Bernasconi, P., Di Blasi, C., Mora, M., Morandi, L., Galbiati, S., Confalonieri, P., Cornelio, F. and Mantegazza, R. (1999) Transforming growth factor-beta1 and fibrosis in congenital muscular dystrophies. *Neuromuscular Disord.*, **9**, 28–33.
49. Ferrario, C.M. (2011) ACE2: more of Ang-(1-7) or less Ang II? *Curr. Opin. Nephrol. Hypertens.*, **20**, 1–6.
50. Zhou, L., Wang, L., Lu, L., Jiang, P., Sun, H. and Wang, H. (2012) Inhibition of miR-29 by TGF-beta-Smad3 signaling through dual mechanisms promotes transdifferentiation of mouse myoblasts into myofibroblasts. *PLoS One*, **7**, e33766.
51. Wang, L., Zhou, L., Jiang, P., Lu, L., Chen, X., Lan, H., Guttridge, D.C., Sun, H. and Wang, H. (2012) Loss of miR-29 in myoblasts contributes to dystrophic muscle pathogenesis. *Mol. Ther.*, **20**, 1222–1233.
52. Serrano, A.L., Mann, C.J., Vidal, B., Ardite, E., Perdiguero, E. and Munoz-Canoves, P. (2011) Cellular and molecular mechanisms regulating fibrosis in skeletal muscle repair and disease. *Curr. Top. Dev. Biol.*, **96**, 167–201.
53. Walther, T., Balschun, D., Voigt, J.P., Fink, H., Zuschratter, W., Birchmeier, C., Ganten, D. and Bader, M. (1998) Sustained long term potentiation and anxiety in mice lacking the Mas protooncogene. *J. Biol. Chem.*, **273**, 11867–11873.
54. De Luca, A., Nico, B., Liantonio, A., Didonna, M.P., Fraysse, B., Pierno, S., Burdi, R., Mangieri, D., Rolland, J.F., Camerino, C. *et al.* (2005) A multidisciplinary evaluation of the effectiveness of cyclosporine a in dystrophic mdx mice. *Am. J. Pathol.*, **166**, 477–489.
55. Morales, M.G., Gutierrez, J., Cabello-Verrugio, C., Cabrera, D., Lipson, K.E., Goldschmeding, R. and Brandan, E. (2013) *Hum. Mol. Genet.*, **22**, 4938–4951.
56. Morales, G., Cabello-Verrugio, C., Cabrera, D., Goldschmeding, R. and Brandan, E. (2011) CTGF/CCN-2 overexpression can directly induce features of skeletal muscle dystrophy. *J. Pathol.*, **225**, 490–501.
57. Li, Y., Foster, W., Deasy, B.M., Chan, Y., Prisk, V., Tang, Y., Cummins, J. and Huard, J. (2004) Transforming growth factor-beta1 induces the differentiation of myogenic cells into fibrotic cells in injured skeletal muscle: a key event in muscle fibrogenesis. *Am. J. Pathol.*, **164**, 1007–1019.
58. Silahtaroglu, A.N., Nolting, D., Dyrskjot, L., Berezikov, E., Moller, M., Tommerup, N. and Kauppinen, S. (2007) Detection of microRNAs in frozen tissue sections by fluorescence in situ hybridization using locked nucleic acid probes and tyramide signal amplification. *Nat. Protoc.*, **2**, 2520–2528.